Acta Mechanica Solida Sinica
https://doi.org/10.1007/s10338-018-0042-6
ISSN 1860-2134

The Dynamic Behaviors of a Shape Memory Polymer Membrane

Yunxin Li[1] **Ruoxuan Liu**[1] **Zishun Liu**[1*]
([1] *International Center for Applied Mechanics, State Key Laboratory for Strength and Vibration of Mechanical Structures, School of Aerospace, Xi'an Jiaotong University, Xi'an 710049, China*)

Received 7 April 2018; revision received 26 July 2018; Accepted 30 July 2018

ABSTRACT As a kind of popular smart materials, shape memory polymers (SMPs) have a great potential for applications in deployable aerospace structures and other engineering structures. However, the vibration analysis of shape memory polymer structures, which would play an important role in engineering, has not gained much attention. In this study, we propose a dynamic model and establish the governing equations for characterizing the dynamic behavior of a shape memory polymer membrane subjected to time-dependent forces. The derivation of governing equations is based on a well-developed constitutive model of SMPs combined with the Euler–Lagrange equation. With the proposed model, two different loading cases are studied: the equal-biaxial sinusoidal force and the uniaxial sinusoidal force. To analyze the dynamic response of a shape memory polymer membrane and find some effective ways to control vibration, the isothermal amplitude–frequency response, the time-dependent behavior of vibration and the vibration in a variable temperature process are investigated in the numerical simulation. It is observed that temperature, mechanical force and heating rate have significant effects on the dynamic performances of a shape memory polymer membrane. We also investigate the shape memory behavior of SMP membrane involving the dynamic response. The influence of dynamics on shape fixation and shape recovery is discussed. These results and discussion may provide guidance for exploring the vibration and dynamic performances of shape memory polymer in deployable aerospace structures.

KEY WORDS Shape memory polymer, Nonlinear vibration, Dynamic model, Thermomechanical behavior

1. Introduction

Shape memory polymers (SMPs) are a new type of smart materials [1–3] which have the capability of returning from a temporary shape to their permanent shape with external stimulus, such as heat [4], magnetic field [5], light [6], electricity [7] and solution [8]. As a new member of the shape memory materials, SMPs have unique properties of lightweight, excellent manufacturability, biodegradability, highly flexible programming, biocompatibility and low cost [9, 10]. With these special characteristics, the applications and potential uses of SMPs have been developed for various areas including aerospace [11–13], biomedicine [14, 15] and textile fabric [16, 17].

* Corresponding author. E-mail:zishunliu@mail.xjtu.edu.cn

Published online: 03 August 2018

Currently, the designs and applications of SMPs in aerospace engineering are mainly focused on deployable aerospace structures such as flexible solar panels. SMPs' lightweight and large recoverable deformation permit important potential applications in flexible solar panels [18, 19]. As an important part of the satellites, flexible solar panels continually serve in space environment with small resistance. The cosmic wind and high-energy particles from environment would cause vibration of the flexible solar panels. Also, because of the large area, small weight and large flexibility of flexible solar panels themselves, vibration of the system could be one of the key factors influencing the normal operation for satellites. Coupled with the special nature of SMP materials, the vibration control of plate-like aerospace SMP structures becomes technically challenging, bursting out the necessity of vibration analysis for such SMP structures. Therefore, recently there has been a great deal of studies on the vibration analysis of space plate structures [20–22]. Although researchers have paid much attention to the investigation of SMP materials [23–25], it appears that results in the vibration analyses of SMP structures are insufficient.

In this work, a dynamic model based on a simplified viscoelastic constitutive model [26] and the Euler–Lagrange equation is developed to predict the dynamic behavior of an SMP membrane. With the proposed model, we investigate the isothermal amplitude–frequency response, the time-dependent behavior of vibration and the vibration in a variable temperature process of an SMP membrane under two different loading cases (equal-biaxial sinusoidal force and uniaxial sinusoidal force), respectively. Then, the effects of temperature, mechanical force and heating rate on the dynamic performances are investigated through the discussion of the simulated results.

With the understanding of shape memory behavior and the dynamic performances of SMP membrane, we further study the shape memory behavior of SMP membrane involving the dynamic response. The influence of dynamics on shape fixation and shape recovery is analyzed.

It should be noted that due to the limitation of the introduced constitutive model, this study is restricted to small strain. For the soft material SMP, the proposed dynamic model is in an early stage. Future work is needed to expand this work to finite strain and large rotation behavior.

The paper is organized as follows. In Sect. 2, we first briefly introduce our simplified viscoelastic constitutive model [26], which agrees well with the experiments, to describe the thermomechanical behavior of SMP structure. Then, we derive the governing equations for an SMP membrane by the Euler–Lagrange equation. In Sect. 3, we reproduce the shape memory behavior of SMPs with the proposed constitutive model. According to the derived governing equations, the numerical simulation results and discussion of the dynamic system are presented in Sect. 4. In these results and discussion, we investigate the factors affecting vibration behavior and present some recommendations for vibration control. In Sect. 5, the shape memory behavior of SMP membrane involving the dynamic response is investigated. Finally, we draw concluding remarks in Sect. 6.

2. Dynamics Model of an SMP Membrane

2.1. Constitutive Model for Shape Memory Polymers

Before the nonlinear dynamic analysis of SMP structure, a simplified viscoelastic constitutive model [26] which is adopted to describe the thermomechanical behavior of SMP structure is briefly introduced here. For a detailed description of this constitutive modeling frame, readers can refer to the reference of Li et al. [26].

The simplified viscoelastic constitutive model, as shown in Fig. 1, consists of three elements: two elastic springs and one dashpot. The one-dimensional constitutive equation for the model is given as follows:

$$\sigma + \frac{\mu\left(T\right)}{\left[E_1\left(T\right)+E_2\left(T\right)\right]}\frac{\mathrm{d}\sigma}{\mathrm{d}t}=\frac{\mu\left(T\right)}{\left[1+E_1\left(T\right)/E_2\left(T\right)\right]}\frac{\mathrm{d}\varepsilon}{\mathrm{d}t}+\frac{1}{\left[1/E_1\left(T\right)+1/E_2\left(T\right)\right]}\varepsilon \tag{1}$$

where $E_1\left(T\right)$ and $E_2\left(T\right)$ are temperature-dependent elastic moduli of the two springs, $\mu\left(T\right)$ is apparent viscosity of the dashpot which also varies with temperature, and σ and ε are, respectively, total stress and total strain. And ε is given as:

$$\varepsilon = \varepsilon_{\mathrm{M}} + \varepsilon_{\mathrm{T}} \tag{2}$$

where ε_{M} is the mechanical strain, $\varepsilon_{\mathrm{T}} = \alpha\left(T - T_0\right)$ is the thermal strain, T_0 is the reference temperature, and α is the thermal expansion coefficient.

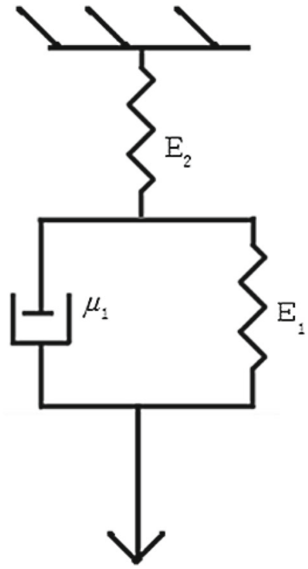

Fig. 1. Schematic of simplified three-element model for SMPs

Equation (1) can be generalized to the 3-D case at small strain as follows:

$$\begin{aligned}
\sigma_x + \tilde{\nu}(T)\frac{\mathrm{d}\sigma_x}{\mathrm{d}t} &= \lambda(T)\left[\varepsilon_{\mathrm{V}} - 3\alpha(T-T_0)\right] + 2\mu(T)\left[\varepsilon_x - \alpha(T-T_0)\right] \\
&\quad + \tilde{\lambda}(T)\left(\frac{\mathrm{d}\varepsilon_{\mathrm{V}}}{\mathrm{d}t} - 3\alpha\frac{dT}{\mathrm{d}t}\right) + 2\tilde{\mu}(T)\left(\frac{\mathrm{d}\varepsilon_x}{\mathrm{d}t} - \alpha\frac{dT}{\mathrm{d}t}\right) \\
\sigma_y + \tilde{\nu}(T)\frac{\mathrm{d}\sigma_y}{\mathrm{d}t} &= \lambda(T)\left[\varepsilon_{\mathrm{V}} - 3\alpha(T-T_0)\right] + 2\mu(T)\left[\varepsilon_y - \alpha(T-T_0)\right] \\
&\quad + \tilde{\lambda}(T)\left(\frac{\mathrm{d}\varepsilon_{\mathrm{V}}}{\mathrm{d}t} - 3\alpha\frac{\mathrm{d}T}{\mathrm{d}t}\right) + 2\tilde{\mu}(T)\left(\frac{\mathrm{d}\varepsilon_y}{\mathrm{d}t} - \alpha\frac{\mathrm{d}T}{\mathrm{d}t}\right) \\
\sigma_z + \tilde{\nu}(T)\frac{\mathrm{d}\sigma_z}{\mathrm{d}t} &= \lambda(T)\left[\varepsilon_{\mathrm{V}} - 3\alpha(T-T_0)\right] + 2\mu(T)\left[\varepsilon_z - \alpha(T-T_0)\right] \\
&\quad + \tilde{\lambda}(T)\left(\frac{\mathrm{d}\varepsilon_{\mathrm{V}}}{\mathrm{d}t} - 3\alpha\frac{dT}{\mathrm{d}t}\right) + 2\tilde{\mu}(T)\left(\frac{\mathrm{d}\varepsilon_z}{\mathrm{d}t} - \alpha\frac{\mathrm{d}T}{\mathrm{d}t}\right) \\
\sigma_{xy} + \tilde{\nu}(T)\frac{\mathrm{d}\sigma_{xy}}{\mathrm{d}t} &= \mu(T)\gamma_{xy} + \tilde{\mu}(T)\frac{\mathrm{d}\gamma_{xy}}{\mathrm{d}t} \\
\sigma_{yz} + \tilde{\nu}(T)\frac{\mathrm{d}\sigma_{yz}}{\mathrm{d}t} &= \mu(T)\gamma_{yz} + \tilde{\mu}(T)\frac{\mathrm{d}\gamma_{yz}}{\mathrm{d}t} \\
\sigma_{zx} + \tilde{\nu}(T)\frac{\mathrm{d}\sigma_{zx}}{\mathrm{d}t} &= \mu(T)\gamma_{zx} + \tilde{\mu}(T)\frac{\mathrm{d}\gamma_{zx}}{\mathrm{d}t}
\end{aligned} \tag{3}$$

where $\varepsilon_{\mathrm{V}} = \varepsilon_x + \varepsilon_y + \varepsilon_z$ is the volumetric strain, $\mu(T)$, $\tilde{\mu}(T)$, $\tilde{\nu}(T)$, $\lambda(T)$ and $\tilde{\lambda}(T)$ are the temperature-dependent material parameters, which can be obtained from $E_1(T)$, $E_2(T)$, $\mu(T)$ and Poisson's ratio ν [26].

The relationship between $E_1(T)$, $E_2(T)$, $\mu(T)$ and temperature is expressed as:

$$E = E_{\mathrm{g}} \exp\left[a_E\left(\frac{T_{\mathrm{g}}}{T} - 1\right)\right] \tag{4}$$

$$\tau = \tau_{\mathrm{g}} \exp\left[a_\tau\left(\frac{T_{\mathrm{g}}}{T} - 1\right)\right] \tag{5}$$

$$\mu = \mu_{\mathrm{g}} \exp\left[a_\mu\left(\frac{T_{\mathrm{g}}}{T} - 1\right)\right] \tag{6}$$

where E_g, τ_g and μ_g are elastic modulus, retardation time and viscosity of material at glass transition temperature T_g, respectively. They can be obtained from experiments such as the dynamic mechanical analysis (DMA) testing. a_E, a_τ and a_μ are constant parameters.

2.2. Governing Equations of Motion for an SMP Membrane

To study the dynamic behaviors of plate-like aerospace SMP structures, a simplified square SMP membrane structure (a typical aerospace structure) is analyzed. The governing equations for a square SMP membrane subject to a time-dependent force are derived in this subsection.

As illustrated in Fig. 2, the square SMP membrane with dimensions of $2H^*2L^*2L$ in the reference state is assumed, and each material point in the SMP membrane is labeled by the material coordinate (X, Y, Z). In the actuation state, the SMP membrane deforms to $2h^*2l_1^*2l_2$, when the forces P_1 and P_2 are applied in the x and y directions. Due to the deformation, the material point (X, Y, Z) moves to a new position with the coordinate (x, y, z). To simplify the problem, the center point of the square membrane (0, 0, 0) is assumed to be unmoved [27, 28]. Defining the strains as $\varepsilon_x = (l_1 - L)/L$, $\varepsilon_y = (l_2 - L)/L$ and $\varepsilon_z = (h - H)/H$, the motion of the SMP membrane can be written as:

$$x = (1 + \varepsilon_x) X, \quad y = (1 + \varepsilon_y) Y, \quad z = (1 + \varepsilon_z) Z \tag{7}$$

For the thermodynamic system, including the SMP membrane, time-dependent force and temperature field, the kinetic energy T and the free energy Π obey the Euler–Lagrange equation:

$$\frac{\partial \ell}{\partial \varepsilon_i} - \frac{\mathrm{d}}{\mathrm{d}t}\left(\frac{\partial \ell}{\partial \dot{\varepsilon}_i}\right) = 0, \quad \ell = T - \Pi \quad (i = 1, 2) \tag{8}$$

where ℓ is the Lagrange, ε_i denotes two independent strains, and $\dot{\varepsilon}_i$ is the rate of change of ε_i.

According to vibration theory, the kinetic energy T can be expressed as [28]:

$$T = \int_\Omega \frac{1}{2}\rho\left(\dot{x}^2 + \dot{y}^2 + \dot{z}^2\right) \mathrm{d}\Omega \tag{9}$$

where ρ is the density of SMP membrane, Ω is the integration interval, $\dot{x}$, and $\dot{y}$ and $\dot{z}$ are the velocities in three axial directions.

The material of SMP membrane obeys the simplified viscoelastic constitutive model (Fig. 1) as introduced in Sect. 2.1. Thus, the free energy of the thermodynamic system is the sum of the mechanical (elastic) energy, the potential energy induced by time-dependent forces, the thermal energy and the initial free energy of SMP membrane [27–29]:

$$\begin{aligned}\Pi = {} & 8HL^2\left[\frac{1}{2}E_1\left(\varepsilon_{1x}^2 + \varepsilon_{1y}^2 + \varepsilon_{1z}^2\right) + \frac{1}{2}E_2\left(\varepsilon_{2x}^2 + \varepsilon_{2y}^2 + \varepsilon_{2z}^2\right) + \rho c_{d_0}\left(T - T_0 - T\log\frac{T}{T_0}\right)\right] \\ & - 2P_1L(1 + \varepsilon_x) - 2P_2L(1 + \varepsilon_y) + \Pi_0\end{aligned} \tag{10}$$

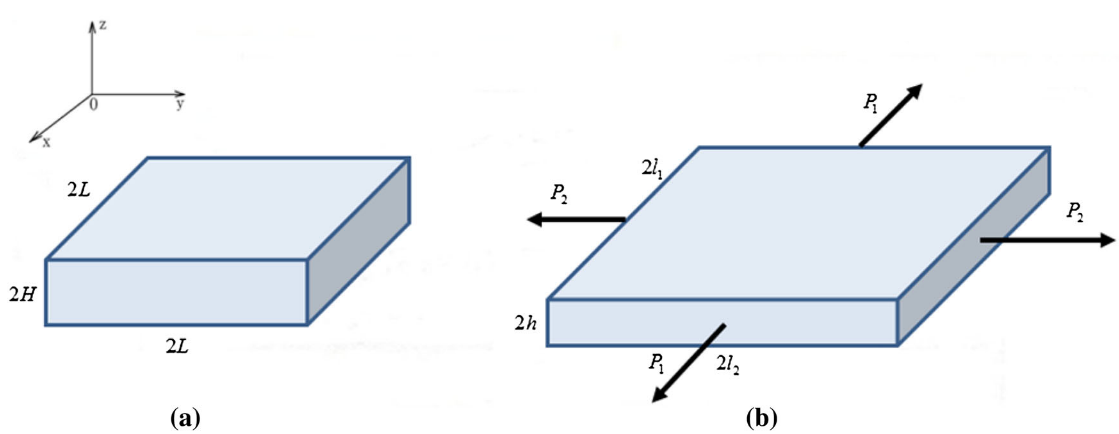

Fig. 2. A square membrane of SMP deforms at two states: **a** in the reference state, there is no force applied to the SMP membrane; **b** in the actuation state, the SMP membrane is subject to a time-dependent force

where ε_{1x}, ε_{1y} and ε_{1z} are strains of spring E_1 in three axial directions; ε_{2x}, ε_{2y} and ε_{2z} are strains of spring E_2 in three axial directions; ε_x and ε_y are the total strains in directions x and y, respectively; Π_0 is the initial free energy, c_{d_0} is the specific heat, and T_0 is the reference temperature.

Considering the SMP as an incompressible material, the Poisson's ratios of two springs are both set as 0.5. For spring E_1, the principal components of the stresses are given by

$$\begin{aligned}\sigma_{1x} &= -p + \frac{2}{3}E_1\varepsilon_{1x}\\ \sigma_{1y} &= -p + \frac{2}{3}E_1\varepsilon_{1y}\\ \sigma_{1z} &= -p + \frac{2}{3}E_1\varepsilon_{1z}\end{aligned} \tag{11}$$

where p is an undetermined pressure. For the actuated SMP membrane (Fig. 2b), there is no stress in direction z, then we have $\sigma_{1z} = 0$. The volumetric strain is zero; thus, $\varepsilon_{1x} + \varepsilon_{1y} + \varepsilon_{1z} = 0$, owing to the incompressibility of material. Then Eq. (11) can be simplified into:

$$\begin{aligned}\sigma_{1x} &= \frac{2}{3}E_1\left(2\varepsilon_{1x} + \varepsilon_{1y}\right)\\ \sigma_{1y} &= \frac{2}{3}E_1\left(2\varepsilon_{1y} + \varepsilon_{1x}\right)\end{aligned} \tag{12}$$

where σ_{1x}, σ_{1y} and ε_{1x}, ε_{1y} are stresses and strains of spring E_1 in directions $x$and$y$, respectively.

Similarly, for spring E_2 and dashpot μ, we obtain:

$$\begin{aligned}\sigma_{2x} &= \frac{2}{3}E_2\left(2\varepsilon_{2x} + \varepsilon_{2y}\right)\\ \sigma_{2y} &= \frac{2}{3}E_2\left(2\varepsilon_{2y} + \varepsilon_{2x}\right)\end{aligned} \tag{13}$$

$$\begin{aligned}\sigma_{\mu x} &= \frac{2}{3}\mu\left(2\dot{\varepsilon}_{\mu x} + \dot{\varepsilon}_{\mu y}\right)\\ \sigma_{\mu y} &= \frac{2}{3}\mu\left(2\dot{\varepsilon}_{\mu y} + \dot{\varepsilon}_{\mu x}\right)\end{aligned} \tag{14}$$

where σ_{2x}, σ_{2y} and $\sigma_{\mu x}$, $\sigma_{\mu y}$ are stresses of spring E_2 and dashpot μ, respectively; ε_{2x} and ε_{2y} are strains of spring E_2; $\dot{\varepsilon}_{\mu x}$ and $\dot{\varepsilon}_{\mu y}$ are the rates of change of dashpot's strains. According to the series and parallel relations of the three elements, the total stresses and total strains can be expressed as:

$$\begin{aligned}\sigma_x &= \sigma_{2x} = \sigma_{1x} + \sigma_{\mu x}\\ \sigma_y &= \sigma_{2y} = \sigma_{1y} + \sigma_{\mu y}\end{aligned} \tag{15}$$

$$\begin{aligned}\varepsilon_x &= \varepsilon_{2x} + \varepsilon_{1x} + \varepsilon_{\mathrm{T}}\\ \varepsilon_y &= \varepsilon_{2y} + \varepsilon_{1y} + \varepsilon_{\mathrm{T}}\end{aligned} \tag{16}$$

where σ_x and σ_y are the total stresses in directions x and y, respectively. The strains of spring E_1 are equal to the dashpot's strains so that $\varepsilon_{\mu x} = \varepsilon_{1x}$ and $\varepsilon_{\mu y} = \varepsilon_{1y}$.

Inserting Eqs. (12–14) into Eqs. (15) and (16), we have:

$$\begin{aligned}E_2\left(2\varepsilon_x - 2\varepsilon_{1x} + \varepsilon_y - \varepsilon_{1y}\right) &= E_1\left(2\varepsilon_{1x} + \varepsilon_{1y}\right) + \mu\left(2\dot{\varepsilon}_{1x} + \dot{\varepsilon}_{1y}\right) + 3E_2\varepsilon_{\mathrm{T}}\\ E_2\left(2\varepsilon_y - 2\varepsilon_{1y} + \varepsilon_x - \varepsilon_{1x}\right) &= E_1\left(2\varepsilon_{1y} + \varepsilon_{1x}\right) + \mu\left(2\dot{\varepsilon}_{1y} + \dot{\varepsilon}_{1x}\right) + 3E_2\varepsilon_{\mathrm{T}}\end{aligned} \tag{17}$$

When the force P varies with time, the dynamic responses of the SMP membrane are complex. The characteristics of loading model also have a significant impact on the behaviors. To study the complex nonlinear vibration of the SMP membrane under the time-dependent force, two in-plane loading models, including the equal-biaxial sinusoidal force ($P_1 = P_2 = P_0\sin\left(2\pi ft\right)$) and the uniaxial sinusoidal force ($P_1 = P_0\sin\left(2\pi ft\right), P_2 = 0$), are applied to the SMP membrane, where P_0 is the amplitude of the force and f is the frequency of excitation.

For equal-biaxial force ($P_1 = P_2 = P$), the total strains are $\varepsilon_x = \varepsilon_y = \varepsilon_{\mathrm{EB}}$, and the strains of spring E_1 are $\varepsilon_{1x} = \varepsilon_{1y} = \varepsilon_{\mathrm{eb}}$. From Eq. (17), the relationship between $\varepsilon_{\mathrm{EB}}$ and $\varepsilon_{\mathrm{eb}}$ can be given as:

$$E_2\varepsilon_{\mathrm{EB}} = \left(E_1 + E_2\right)\varepsilon_{\mathrm{eb}} + E_2\varepsilon_{\mathrm{T}} + \mu\dot{\varepsilon}_{\mathrm{eb}} \tag{18}$$

The kinetic energy of SMP membrane can be obtained from Eq. (9):

$$T=\frac{8}{3}\rho L^4 H\dot{\varepsilon}_{\mathrm{EB}}^2+\frac{4}{3}\rho L^2 H^3\left(2\dot{\varepsilon}_{\mathrm{EB}}-3\dot{\varepsilon}_{\mathrm{T}}\right)^2 \tag{19}$$

and the free energy is derived from Eq. (10):

$$\begin{aligned}\mathit{\Pi}=8HL^2&\left[3E_1\varepsilon_{\mathrm{eb}}^2+3E_2\left(\varepsilon_{\mathrm{EB}}-\varepsilon_{\mathrm{eb}}-\varepsilon_{\mathrm{T}}\right)^2+\rho c_{d_0}\left(T-T_0-T\log\frac{T}{T_0}\right)\right]\\&-4PL\left(1+\varepsilon_{\mathrm{EB}}\right)+\mathit{\Pi}_0\end{aligned} \tag{20}$$

Substituting Eqs. (19) and (20) into Eq. (8), the governing equation for the equal-biaxial force case is:

$$\begin{aligned}&\left(\frac{16}{3}\rho L^4 H+\frac{32}{3}\rho L^2 H^3\right)\ddot{\varepsilon}_{\mathrm{EB}}-16\rho L^2 H^3\ddot{\varepsilon}_{\mathrm{T}}\\&+48HL^2\cdot\left[\frac{E_1E_2}{E_1+E_2}\left(\varepsilon_{\mathrm{EB}}-\varepsilon_{\mathrm{T}}\right)\right]-4PL=0\end{aligned} \tag{21}$$

For uniaxial force ($P_1=P$, $P_2=0$), the total strain in direction x is $\varepsilon_x=\varepsilon_{UA1}$ and in direction y is $\varepsilon_y=\varepsilon_{UA2}$, and the strains of spring E_1 are $\varepsilon_{1x}=\varepsilon_{ua1}$, $\varepsilon_{1y}=\varepsilon_{ua2}=-0.5\varepsilon_{ua1}$. Based on the condition of uniaxial force, Eq. (17) can be simplified as:

$$E_2\varepsilon_{UA1}=\left(E_1+E_2\right)\varepsilon_{ua1}+2E_2\varepsilon_{\mathrm{T}}+\mu\dot{\varepsilon}_{ua1} \tag{22}$$

Similarly, in Eqs. (19) and (20), the kinetic energy and the free energy under the condition of uniaxial force are obtained as follows:

$$T=\frac{4}{3}\rho L^4 H\dot{\varepsilon}_{UA1}^2+\frac{1}{3}\rho L^4 H\left(\dot{\varepsilon}_{UA1}-3\dot{\varepsilon}_{\mathrm{T}}\right)^2+\frac{1}{3}\rho L^2 H^3\left(2\dot{\varepsilon}_{UA1}-3\dot{\varepsilon}_{\mathrm{T}}\right)^2 \tag{23}$$

$$\begin{aligned}\mathit{\Pi}=8HL^2&\left\{\frac{1}{2}E_2\left[\left(\varepsilon_{UA1}-\varepsilon_{ua1}-\varepsilon_{\mathrm{T}}\right)^2+\left(-\frac{1}{2}\varepsilon_{UA1}+\frac{1}{2}\varepsilon_{ua1}-\varepsilon_{\mathrm{T}}\right)^2+\left(\frac{1}{2}\varepsilon_{UA1}-\frac{1}{2}\varepsilon_{ua1}-\varepsilon_{\mathrm{T}}\right)^2\right]\right.\\&\left.+\frac{3}{4}E_1\varepsilon_{ua1}^2+\rho c_{d_0}\left(T-T_0-T\log\frac{T}{T_0}\right)\right\}-2PL\left(1+\varepsilon_{UA1}\right)+\mathit{\Pi}_0\end{aligned} \tag{24}$$

Substituting Eqs. (23) and (24) into Eq. (8), the governing equation for the uniaxial force case is:

$$\begin{aligned}&\left(\frac{10}{3}\rho L^4 H+\frac{2}{3}\rho L^2 H^3\right)\ddot{\varepsilon}_{UA1}-2\left(\rho L^4 H+\rho L^2 H^3\right)\ddot{\varepsilon}_{\mathrm{T}}\\&+12HL^2\cdot\left[\frac{E_1E_2}{E_1+E_2}\left(\varepsilon_{UA1}-\varepsilon_{\mathrm{T}}\right)\right]-2PL=0\end{aligned} \tag{25}$$

To sum up, the dynamics model of an SMP membrane has been developed by a thermomechanical constitutive model and the Euler–Lagrange equation. Equations (21) and (25), which govern the evolution of the time-dependent strains of the specific material structure, are used in the following analysis to study the dynamic response of an SMP membrane in the equal-biaxial force case and the uniaxial force case, respectively.

3. Constitutive Model Verification

To verify whether the constitutive model presented in Sect. 2.1 can predict the shape memory behavior of SMPs, we simulate the thermomechanical tests of an SMP reported by Tobushi et al. [4]. The material parameters of SMP are $E_{\mathrm{g}}=146$ MPa, $a_E=38.1$, $\tau_{\mathrm{g}}=521$ s, $a_\tau=35.4$, $\mu_{\mathrm{g}}=14$ GPa·s, $a_\mu=44.2$, $\rho=1005$ kg/m^3, $T_{\mathrm{g}}=328$ K, and $\alpha=11.6\times10^{-5}$ K^{-1}. There are two typical cases of shape memory behavior: free recovery circle and constraint recovery circle. Figure 3a, b illustrates the stress–temperature curves and the strain–temperature curves in free recovery circle. Figure 3c, d shows the stress–temperature curves and the stress–strain curves in constraint recovery circle. The simulated results are compared with the experiments and good agreement is observed. Thus, this constitutive model can capture the key features of SMPs. It is reasonable to use this model in the subsequent studies.

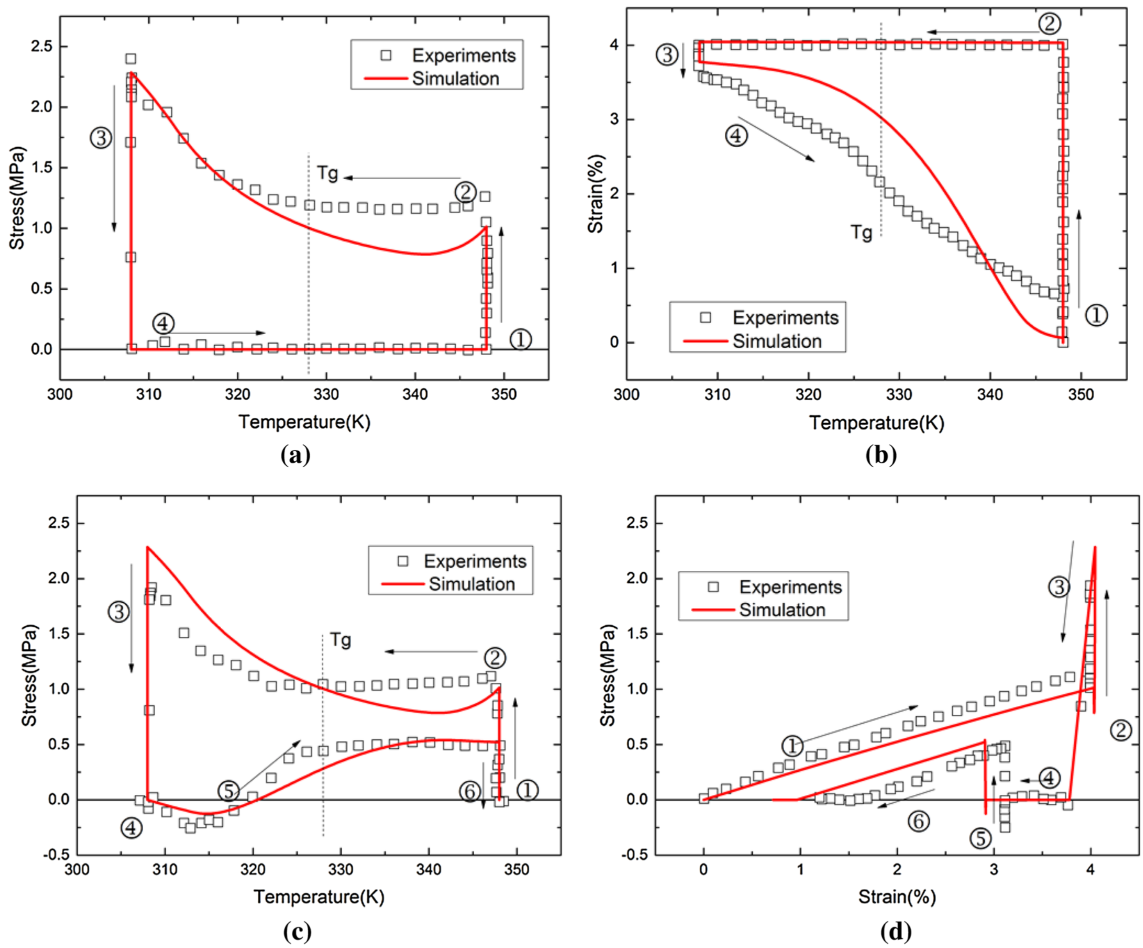

Fig. 3. Comparisons between the experiments and the calculated results for shape memory behavior: **a** the stress–temperature curves in free recovery circle; **b** the strain–temperature curves in free recovery circle; **c** the stress–temperature curves in constraint recovery circle; **d** the stress–strain curves in constraint recovery circle

4. Dynamic Response of SMP Membrane

As shown in Fig. 3a, b, a typical shape memory cycle can be divided into four processes. In process ① (loading), the SMP specimen is pre-deformed from the original shape to a pre-deformation state. Then the specimen is cooled to a lower temperature with the pre-deformation or pre-force maintained in process ② (cooling). In process ③ (unloading), the strain- or force-constraint conditions are removed from the specimen and the SMP can retain a temporary shape. And then the deformed SMP is sent to the place where it needs to be used. Followed by the last process (heating), the SMP specimen is reheated to a high temperature and recovered to its original shape. SMP structures will serve in the recovered shape (the original shape) for a long time, e.g., the expanded solar panels. Thus, it is necessary to study the dynamic response of SMP in this state.

Subject to a sinusoidal force ($P = P_0 \sin(2\pi f t)$), the dynamic behaviors of the SMP membrane with two different in-plane loading cases (the equal-biaxial sinusoidal force and the uniaxial sinusoidal force) are investigated in this section. To find the ways to control the vibration of SMP membrane, for both cases, we explore the effects of temperature, mechanical force and excitation frequency on the isothermal dynamic response and the influence of heating rate in temperature-change vibration. We hope that these results and discussion can provide guidance to the exploration in SMPs' vibration and vibration control. We assume that the SMP membrane is activated from the reference state; thus, the initial conditions of Eqs. (21) and (25) are given by $\varepsilon_{\mathrm{EB}} = 0$, $\dot{\varepsilon}_{\mathrm{EB}} = 0$ and $\varepsilon_{UA1} = 0$, $\dot{\varepsilon}_{UA1} = 0$, respectively. In this simulation, the size of the membrane is set as $L = 0.5\,\mathrm{m}$, $H = 0.05\,\mathrm{m}$.

4.1. Equal-Biaxial Sinusoidal Force

4.1.1. Isothermal Dynamic Response of an SMP Membrane

In this subsection, we try to find out the method of controlling vibration of the SMP membrane by studying the main factors that influence vibration. Thus, the isothermal dynamic response of an SMP membrane under the effects of temperature, mechanical force and excitation frequency would be investigated here. Solving Eq. (21) with the initial conditions $\varepsilon_{\mathrm{EB}} = 0$ and $\dot{\varepsilon}_{\mathrm{EB}} = 0$, we can obtain the vibration of an SMP membrane under equal-biaxial sinusoidal force.

As a temperature-sensitive material, SMP's thermomechanical behaviors are different with varying temperatures. Thus, we plot the amplitudes of total strain $\varepsilon_{\mathrm{EB}}$ as functions of the excitation frequency at five different temperatures (as shown in Fig. 4a) to study the influence of temperature. Here, we define the amplitude as half of the difference between the maximal and minimal values of strain. It is observed that both the vibration amplitude of strain and the resonance frequency (where the maximum amplitude appears) of the responses vary with temperature. Specifically, for a given constant $P_0 = 200$ N, as shown in Fig. 4a, the resonance frequency becomes smaller at a higher temperature, while the maximal amplitude increases when temperature increases. As shown in Fig. 4b, we also plot the amplitude–frequency response of an SMP membrane for a constant temperature $T = 343$ K and three different P_0. When the temperature remains constant, the maximal amplitude increases with the increase of P_0, while the resonance frequency barely changes. To further understand these phenomena in Fig. 4a, we plot the resonance frequency as function of temperature in linear coordinates and semi-log coordinates, respectively, as shown in Fig. 5. Figure 5a shows that there is no obvious regularity between resonance frequency and temperature in the linear coordinate diagram. However, resonance frequency and temperature develop a linear relationship in the semi-log coordinate diagram, due to the approximate delineation of relationship between elastic modulus and temperature by Eq. (4) [4]. The linear relationship of resonance frequency versus temperature (Fig. 5) can be used to control the vibration of the SMP membrane. When the working temperature of the SMP membrane is given, the resonance frequency of the membrane at this temperature can be deduced from Fig. 5. Then, we can intentionally avoid the resonance frequency to prevent the resonance from happening. Also, when the frequency of excitation (f) is known, the resonance can be avoided by controlling the temperature of SMP membrane.

To study the effect of excitation frequency on the isothermal dynamic response, the time-dependent behaviors of vibration at different temperatures are illustrated in Fig. 6. For each temperature, three levels of excitation frequencies, i.e., the resonant frequency (blue curves), half of the resonant frequency (red curves) and double of the resonant frequency (black curves), are chosen. It can be seen that the

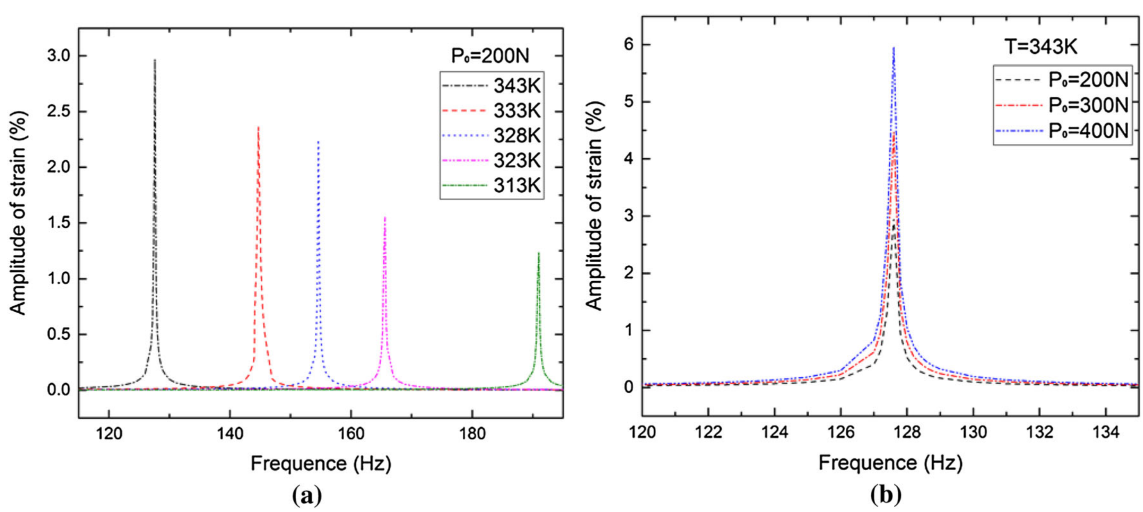

Fig. 4. Isothermal amplitude–frequency response of an SMP membrane under equal-biaxial sinusoidal force: **a** for a constant $P_0 = 200\,\mathrm{N}$ and five different temperatures; **b** for a constant temperature $T = 343\,\mathrm{K}$ and three different P_0

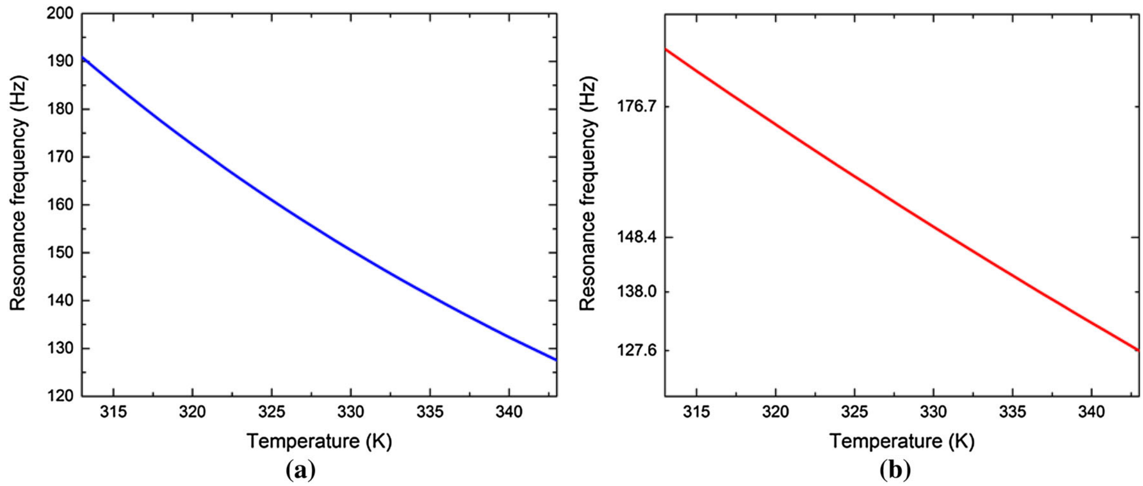

Fig. 5. Resonance frequency–temperature curve: **a** in linear coordinates; **b** in semi-log coordinates

strongest vibration of SMP system occurs when the frequency of excitation is around the resonant frequency. At half of the resonant frequency and double of the resonant frequency, the deformations of $\varepsilon_{\mathrm{EB}}$ are both very small. Furthermore, from the local enlarged drawings in Fig. 6, we can find that the amplitudes of red curves are always bigger than those of black curves. This is because the loading rates can affect the nominal elastic modulus of this viscoelastic material. At a higher excitation frequency, the nominal elastic modulus is larger and the deformations of $\varepsilon_{\mathrm{EB}}$ would be smaller.

4.1.2. Vibration of an SMP Membrane in Temperature-Changing Process: Influence of the Heating Rate

The dynamic behaviors of the SMP membrane shown in Figs. 4, 5 and 6 are all for isothermal vibration cases, because the SMP applications commonly work at certain temperatures. However, the responses of SMP structures are often accompanied by a temperature-changing process. It is imperative to study the vibration of SMP membrane in a variable temperature process. In the following examples, an equal-biaxial sinusoidal force is applied to the SMP membrane at 313 K firstly. And then, we keep the excitation and heat the SMP membrane from 313 to 343 K with a heating rate of 0.0667 K/s [4]. Figure 7 demonstrates the oscillation of $\varepsilon_{\mathrm{EB}}$ during heating under different excitation frequencies. During the heating process, resonance occurs (the oscillation amplitude increases dramatically) in the vicinity of a certain temperature (we call it a resonant-sensitive temperature). However, as the temperature continues to rise, the oscillation amplitude decreases rapidly and resonance disappears. From Fig. 5, we can find that the three excitation frequencies of 165.6 HZ, 154.6 HZ and 144.7 HZ correspond to the resonance frequencies of SMP membrane at 323 K, 328 K and 333 K, respectively. Figure 7 also shows that the temperatures where the resonance occurs are near 323 K, 328 K and 333 K, which are consistent with the results of Fig. 5. In addition, at the same excitation frequency, the maximum amplitudes in this heating process are smaller than those in the isothermal process (Fig. 6). The reason might be that as the heating process is fast, the vibration has not reached the resonant value when the temperature passes the resonant-sensitive temperature. It can be deduced that the vibration of SMP membrane in a heating process is related to the heating rate.

Therefore, we would consider another two heating processes with higher heating rates. Figures 8 and 9 plot the oscillation of $\varepsilon_{\mathrm{EB}}$ during heating with the heating rates of 0.3335 and 0.667 K/s, respectively. As is shown, when the heating rate increases, the maximum values for amplitude become smaller, while the temperatures where resonance occurs barely change. That is to say, in the temperature-changing process, the heating rate affects the maximum amplitude instead of the temperature where resonance occurs. This phenomenon suggests another idea to control the vibration of the SMP membrane. When the frequency of excitation is known, we can heat the SMP membrane rapidly until near the resonant-sensitive temperature, and the maximum amplitude could be much smaller.

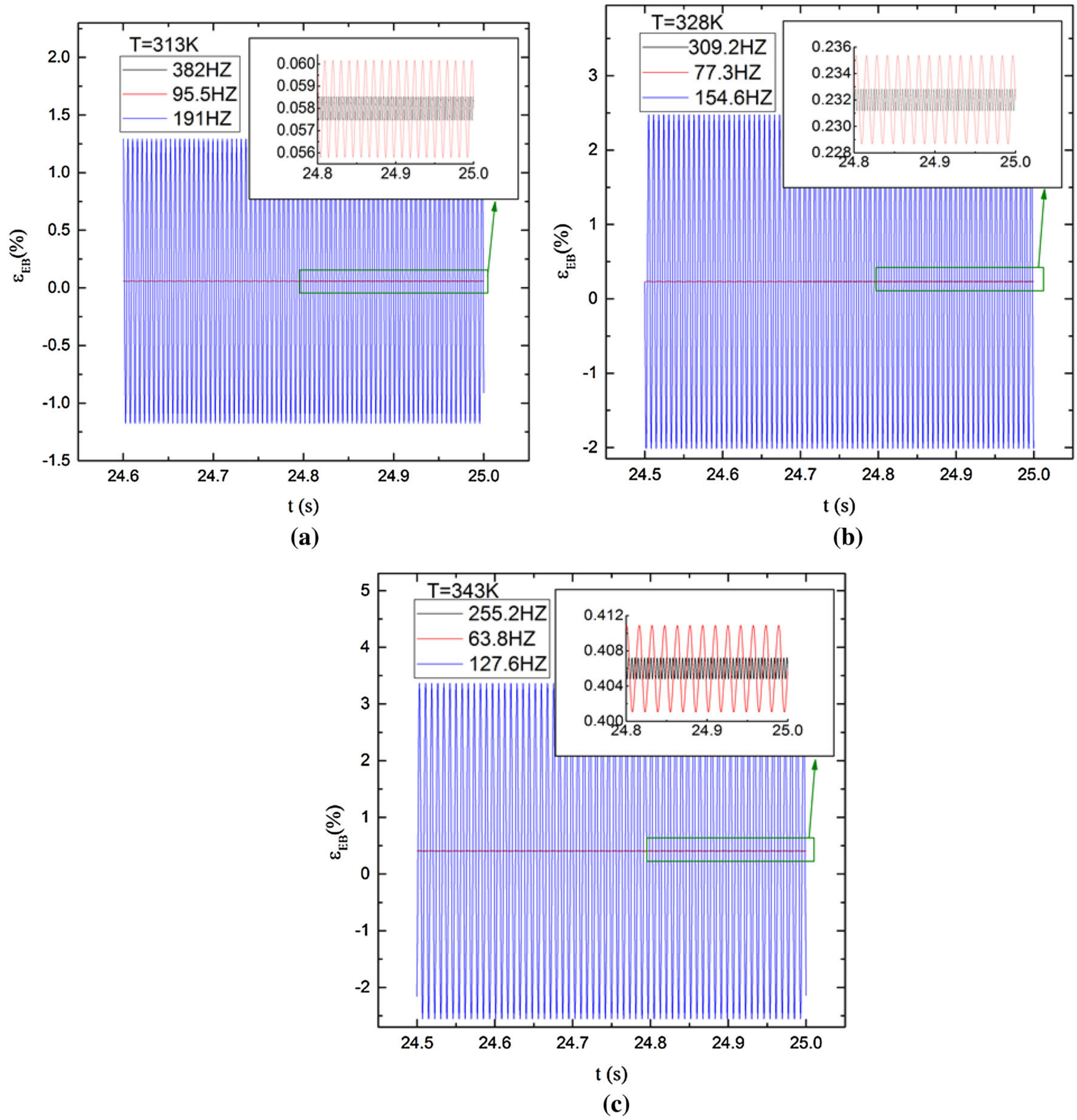

Fig. 6. Time-dependent behaviors of vibration at different temperatures. For each temperature, three levels of excitation frequencies, i.e., the resonant frequency (blue curves), half of the resonant frequency (red curves) and double of the resonant frequency (black curves), are chosen: **a** T=313 K and three excitation frequencies are 191 HZ, 95.5 HZ and 382 HZ, respectively; **b** T=328 K and three excitation frequencies are 154.6 HZ, 77.3 HZ and 309.2 HZ, respectively; **c** T=343 K and three excitation frequencies are 127.6 HZ, 63.8 HZ and 255.2 HZ, respectively

4.2. Uniaxial Sinusoidal Force

4.2.1. Isothermal Dynamic Response of an SMP Membrane

The isothermal dynamic response of an SMP membrane under the effects of temperature, mechanical force and excitation frequency is studied for the uniaxial sinusoidal force case here.

The isothermal amplitude–frequency response is shown in Fig. 10. From Fig. 10a, it can be seen that when $P_0 = 200$ N is maintained and temperature decreases from 343 to 313 K, the value of amplitude peak decreases, and the resonance frequency becomes bigger. The amplitude reaches a maximum peak value of 6.92 at 81.4 HZ for 343 K and a smaller peak value of 2.84 at 121.8 HZ for 313 K. Compared with the condition of equal-biaxial sinusoidal force, at the same temperature, the maximal amplitude

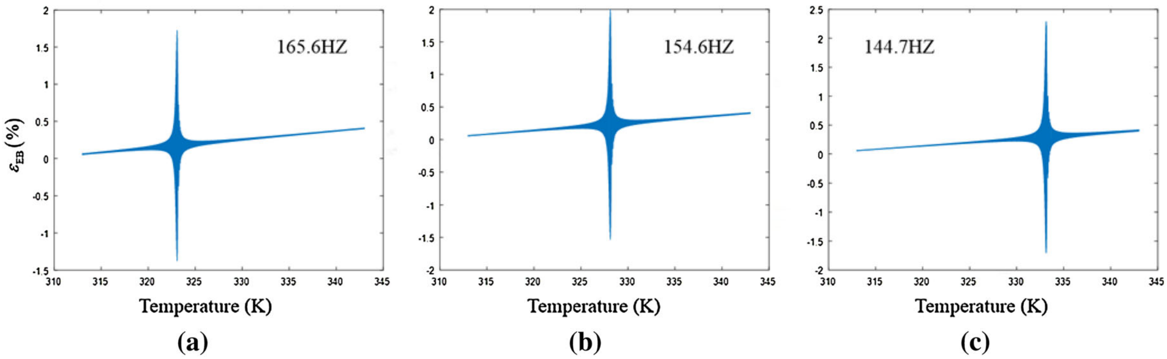

Fig. 7. The oscillation of $\varepsilon_{\mathrm{EB}}$ during heating (at the heating rate of 0.0667 K/s) under different excitation frequencies: **a** f=165.6 HZ; **b** f=154.6 HZ; **c** f=144.7 HZ

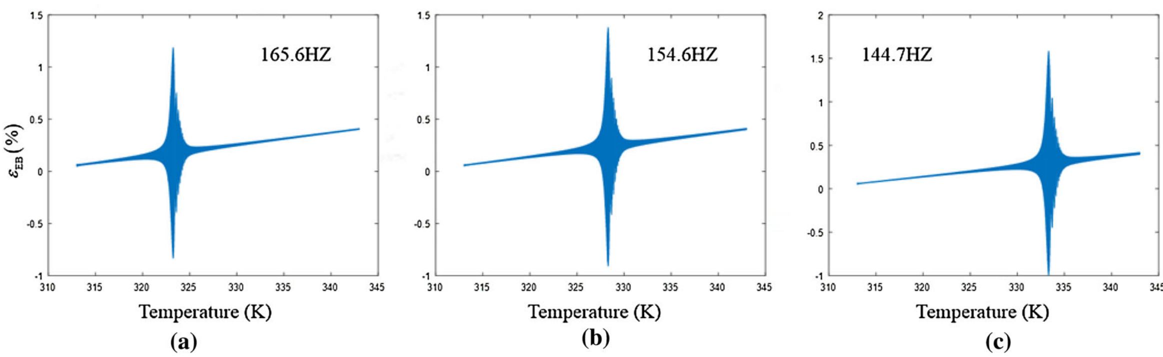

Fig. 8. The oscillation of $\varepsilon_{\mathrm{EB}}$ during heating (at the heating rate of 0.3335 K/s) under different excitation frequencies: **a** f=165.6 HZ; **b** f=154.6 HZ; **c** f=144.7 HZ

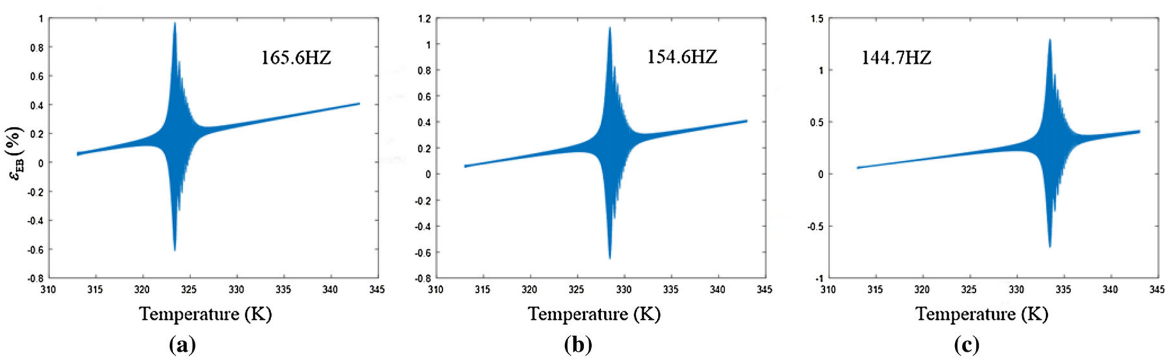

Fig. 9. The oscillation of $\varepsilon_{\mathrm{EB}}$ during heating (at the heating rate of 0.667 K/s) under different excitation frequencies: **a** f=165.6 HZ; **b** f=154.6 HZ; **c** f=144.7 HZ

of SMP membrane under uniaxial sinusoidal force increases and the resonance frequency is smaller. We also compare the amplitude–frequency response under uniaxial sinusoidal force for a constant temperature $T = 343$ K and three different P_0 in Fig. 10b. Similar to the responses of SMP membrane under equal-biaxial sinusoidal force, the maximal amplitude increases with the increase of P_0, while the resonance frequency barely changes. Furthermore, we also plot the relationship between resonance frequency and temperature of SMP membrane under uniaxial sinusoidal force in Fig. 11, which is useful to control the vibration of the SMP membrane.

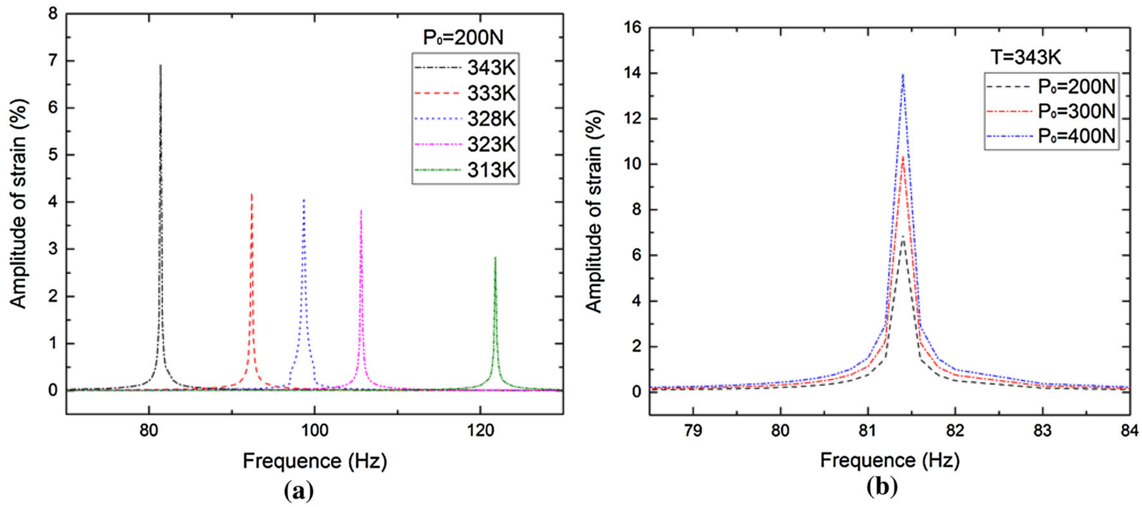

Fig. 10. Isothermal amplitude–frequency response of an SMP membrane under uniaxial sinusoidal force: **a** for a constant force $P_0 = 200$ N and five different temperatures; **b** for a constant temperature $T = 343$ K and three different force P_0

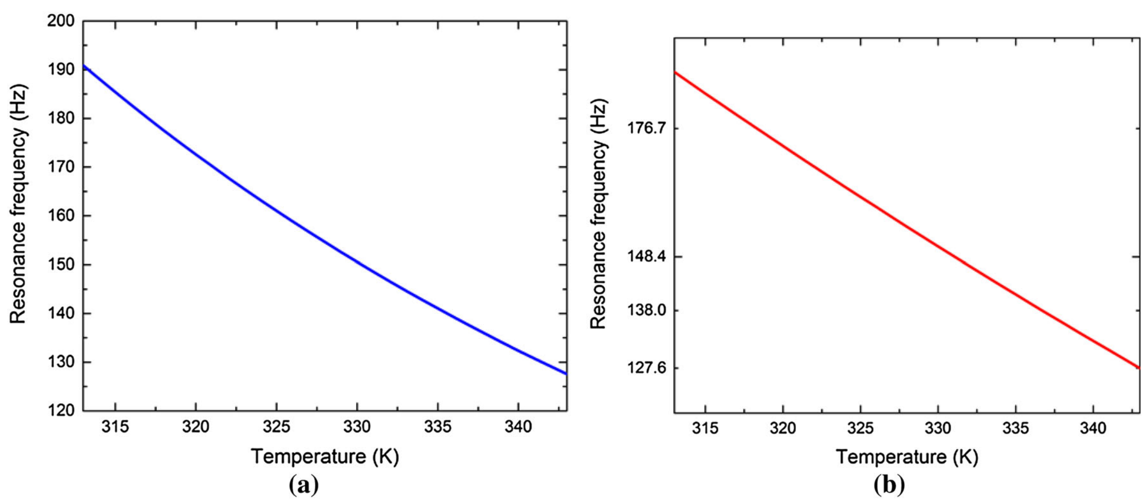

Fig. 11. Resonance frequency–temperature curve of an SMP membrane under uniaxial sinusoidal force: **a** in linear coordinates; **b** in semi-log coordinates

The time history of vibration of an SMP membrane at five different temperatures is shown in Fig. 12. Similar to the case under equal-biaxial sinusoidal force, to inquire into the effect of excitation frequency on the isothermal dynamic response, for each temperature, we choose three levels of excitation frequencies, i.e., the resonant frequency (blue curves), half of the resonant frequency (red curves) and double of the resonant frequency (black curves). The phenomena are the same as those under the condition of equal-biaxial sinusoidal force. The biggest vibration of SMP membrane takes place in the vicinity of the resonant frequency, and the amplitudes of red curves are always bigger than those of black curves due to the same reason explained before. Thus, it's necessary for us to control the vibration of the SMP membrane as well as to avoid the frequency preserve and resonance.

4.2.2. Vibration of an SMP Membrane in Temperature-Changing Process: Influence of the Heating Rate

The oscillations of $\varepsilon_{\mathrm{EB}}$ under uniaxial sinusoidal force during heating with different heating rates of 0.0667 K/s, 0.3335 K/s and 0.667 K/s, are depicted in Figs. 13, 14 and 15, respectively. During

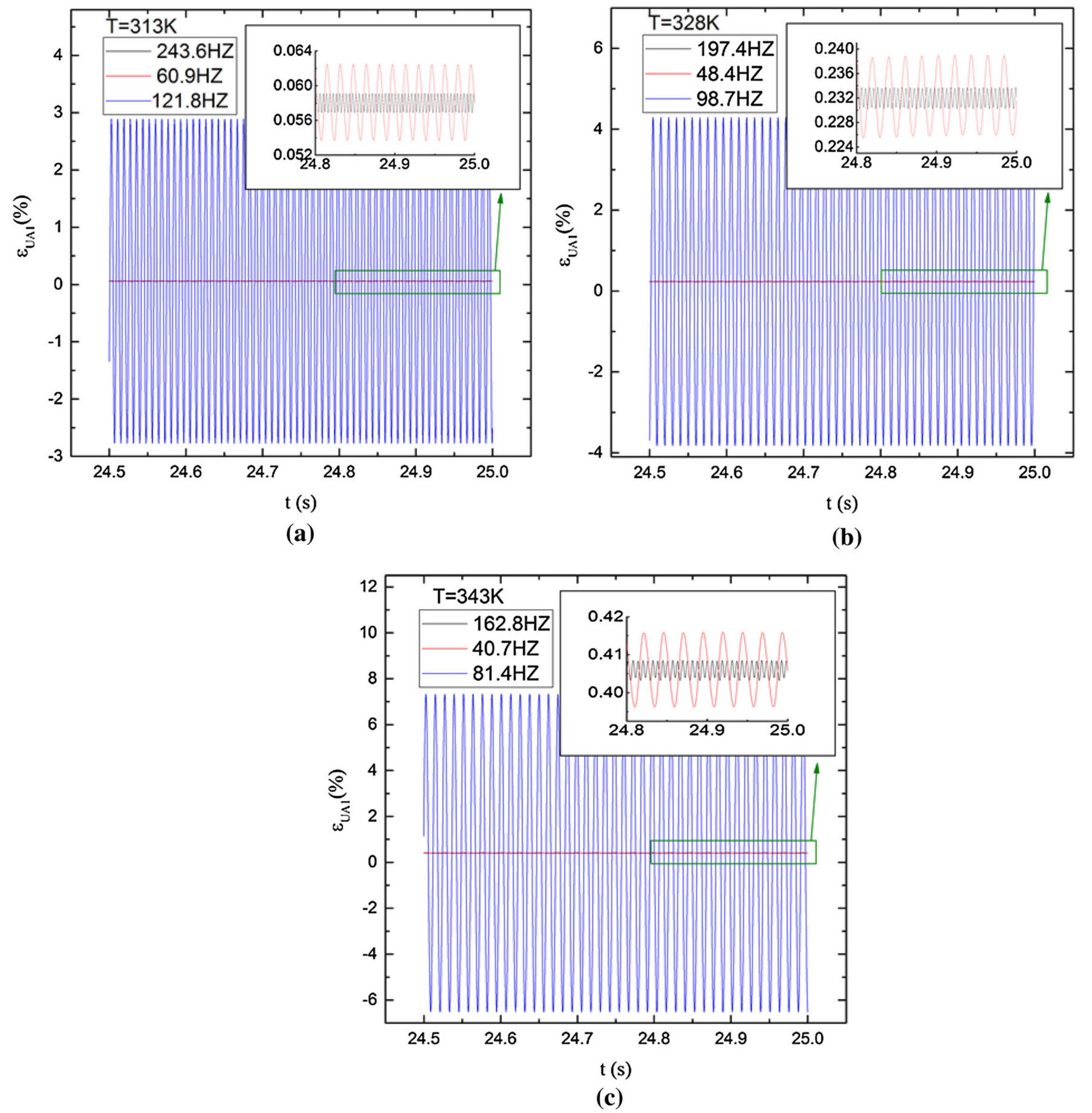

Fig. 12. Time history of vibration under uniaxial sinusoidal force at five different temperatures. For each temperature, three levels of excitation frequencies, i.e., the resonant frequency (blue curves), half of the resonant frequency (red curves) and double of the resonant frequency (black curves), are chosen: **a** T=313 K and three excitation frequencies are 121.8 HZ, 60.9 HZ and 243.6 HZ, respectively; **b** T=328K and three excitation frequencies are 98.7 HZ, 48.4 HZ and 197.4 HZ, respectively; **c** T=343 K and three excitation frequencies are 81.4 HZ, 40.7 HZ and 162.8 HZ, respectively

the heating process, the oscillation amplitude increases dramatically in the vicinity of the resonant-sensitive temperature. When the heating rate increases from 0.0667 to 0.667 K/s, the amplitude peak decreases, while the temperatures where resonance occurs barely change. These are consistent with the results of equal-biaxial sinusoidal force case.

5. Shape Memory Behavior of SMP Membrane Involving the Dynamic Response

We have studied the shape memory behavior of SMP in quasi-static process and the dynamic behavior of a SMP membrane under time-dependent forces in Sects. 3 and 4. However, in the quasi-static shape memory cycle process, there may be some small disturbances or dynamic loads in static loading. Thus, the shape memory behavior of SMP membrane involving the dynamic response should

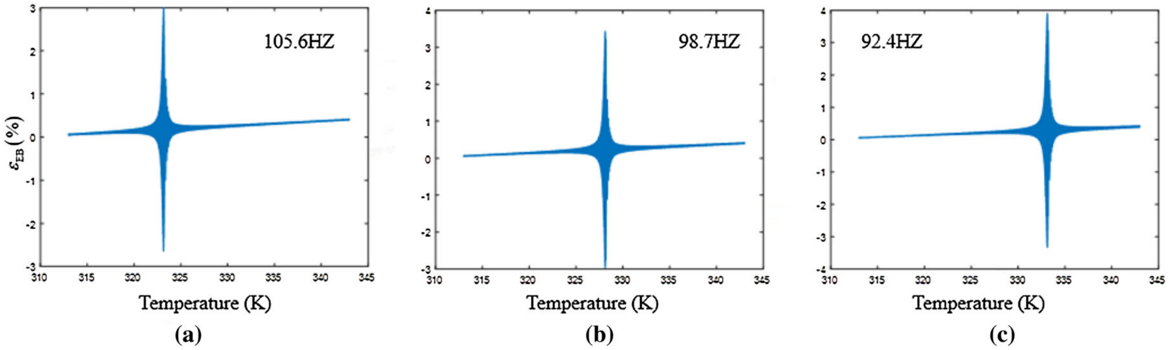

Fig. 13. The oscillation of $\varepsilon_{\mathrm{EB}}$ during heating (at the heating rate of 0.0667 K/s) under uniaxial sinusoidal force with different excitation frequencies: **a** f=105.6 HZ; **b** f=98.7 HZ; **c** f=92.4 HZ

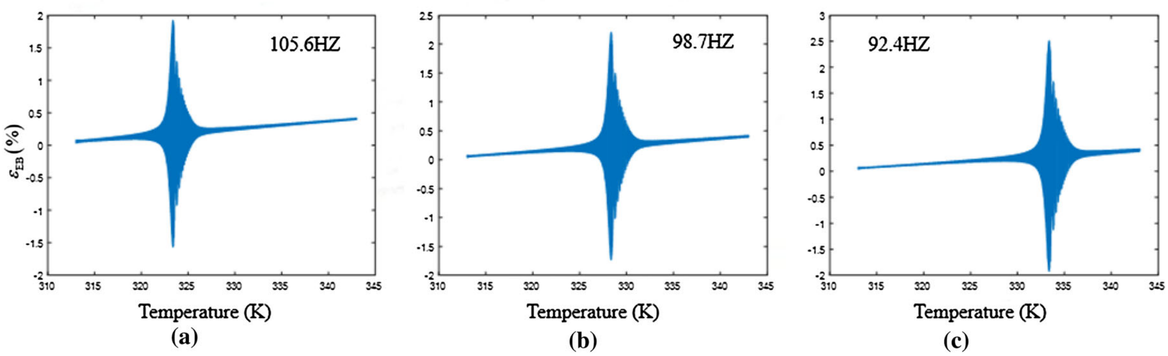

Fig. 14. The oscillation of $\varepsilon_{\mathrm{EB}}$ during heating (at the heating rate of 0.3335 K/s) under uniaxial sinusoidal force with different excitation frequencies: **a** f=105.6 HZ; **b** f=98.7 HZ; **c** f=92.4 HZ

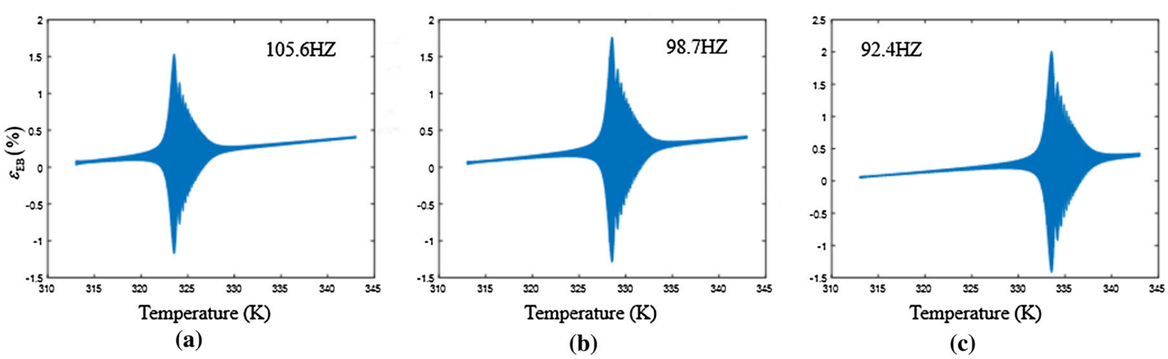

Fig. 15. The oscillation of $\varepsilon_{\mathrm{EB}}$ during heating (at the heating rate of 0.667 K/s) under uniaxial sinusoidal force with different excitation frequencies: **a** f=105.6 HZ; **b** f=98.7 HZ; **c** f=92.4 HZ

be researched. In this section, we would investigate the influence of dynamics on shape fixation and shape recovery, respectively.

5.1. The Influence of Dynamics on Shape Fixation

In the following examples, the SMP membrane is pre-stretched to 5% under an equal-biaxial force at 343 K firstly. Then, the material is cooled to 313 K. In regular shape fixing process, the strain can be stored under the pre-force maintained. To investigate the dynamic response of the SMP membrane in shape fixing process, during the cooling process, a sinusoidal force $P = P_{\mathrm{s}} + P_{\mathrm{d}} \sin(2\pi f t)$ is applied

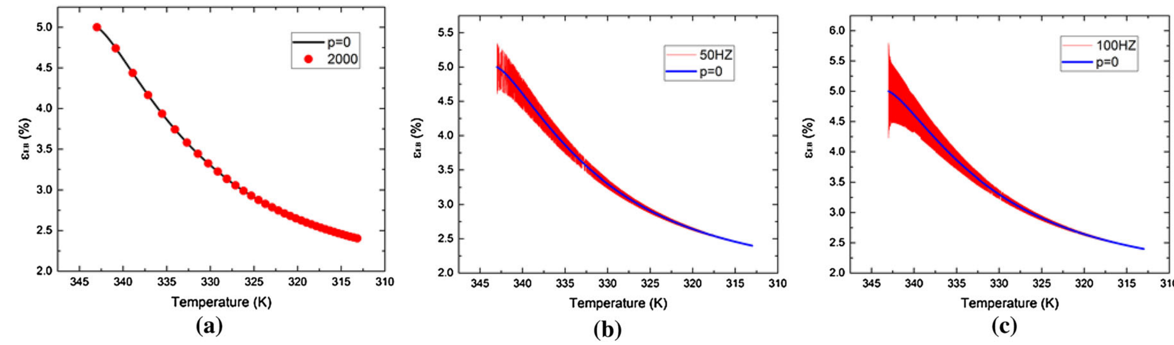

Fig. 16. Strain–temperature curves of the SMP membrane for a given $P_{\rm d} = 2000$ N and different excitation frequencies in the cooling process: **a** $f = 0$ HZ; b $f = 50$ HZ; **c** $f = 100$ HZ

here. $P_{\rm s}$ is the static force, which is equal to the pre-force. $P_{\rm d}$ is the amplitude of dynamic force. f is excitation frequency.

For a given constant $P_{\rm d} = 2000$ N, the simulated strain–temperature curves of the dynamic response for the SMP membrane with different excitation frequencies in shape fixing process are shown in Fig. 16. In order to compare the dynamic response and quasi-static shape fixing process, the regular quasi-static shape fixing process ($P_{\rm d} = 0$ N) is also illustrated in Fig. 16. When $f = 0$ HZ, the force $P = P_{\rm s} + P_{\rm d}$ is static. It can be seen from Fig. 16a that in the static loading cases, the strain–temperature curves of $P_{\rm d} = 0$ N and $P_{\rm d} = 2000$ N are almost coincident. That is to say, a small static load $P_{\rm d}$ has little effect on the original shape fixing process. However, when $f \neq 0$ HZ, as shown in Fig. 16b, c, the strain curves have a noticeable oscillation near the original strain–temperature curve. This oscillation occurs mainly in the early stage of cooling process where the temperature is high and the modulus is low. When f increases from 50 to 100 HZ, the vibration becomes larger. From Fig. 5, we can see that at the temperature range of 313–343 K, the resonance frequencies of the SMP membrane are 128–191 HZ. The excitation frequency $f = 100$ HZ is close to the resonant frequency range; thus, the vibration of this case is more obvious. Such vibration, especially for the resonance at the special frequency, may destroy the material during the cooling process. Then, the shape fixing process can't be completed as expected. But it can be seen that as long as $P_{\rm d}$ is not very large and the vibration does not destroy the material during the cooling process, the freezing strain at the end of cooling is the same. The dynamics have little influence on final shape fixation.

5.2. The Influence of Dynamics on Shape Recovery

In this subsection, we investigate the influence of dynamics on shape recovery in the shape memory cycle. The simulated case can be divided into four processes. The initial processes ① → ② → ③ are the same as those in the free recovery cycle (Fig. 3b). They are all quasi-static processes. In the fourth process, the SMP membrane is reheated to 343 K under an equal-biaxial time-dependent force $P = P_{\rm d} \sin(2\pi f t)$.

Figure 17 plots the strain–temperature curves of the SMP membrane for a given $P_{\rm d} = 2000$ N and different excitation frequencies in the heating process. To compare the dynamic response and quasi-static shape recovery process, the regular free heating recovery process ($P_{\rm d} = 0$N) is also illustrated in Fig. 17. As shown in Fig. 17a, when $f = 0$ HZ, the influence of the small static force ($P = P_{\rm d}$) on shape recovery can be neglected. In the heating process, the strain–temperature curve of the case $f = 0$ HZ overlaps with the curve in the free heating recovery process. Figure 17b, c shows the effect of dynamics on shape recovery. When $f \neq 0$ HZ, a noticeable oscillation can be observed. It is similar to the cooling process, when f increases from 50 HZ to 100 HZ, the vibration becomes larger. The vibration may cause the SMP membrane to deviate from the original desired shape during the shape recovery process and the final invalidation of the material.

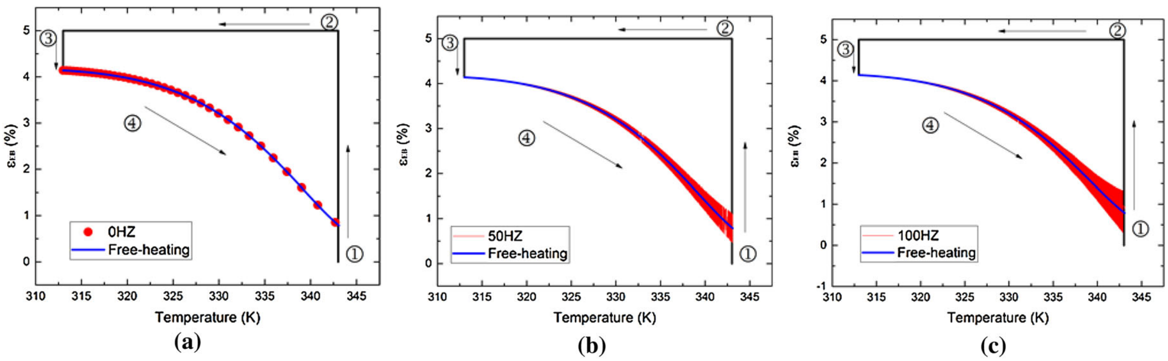

Fig. 17. Strain–temperature curves of the SMP membrane for a given $P_{\mathrm{d}} = 2000$ N and different excitation frequencies in the heating process: **a** $f = 0$ HZ; **b** $f = 50$ HZ; **c** $f = 100$ HZ

6. Conclusion

Based on a thermomechanical constitutive model and the Euler–Lagrange equation, we establish a dynamic model to study the dynamic behaviors of an SMP membrane in two different in-plane loading cases: the equal-biaxial sinusoidal force and the uniaxial sinusoidal force. We find that when the temperature rises, the resonance frequency decreases and the value of amplitude peak increases under an equal-biaxial sinusoidal force. The relationship curve between resonance frequency and temperature provides a useful guidance to control the vibration of SMP membrane. Furthermore, we observe that the time-dependent dynamic response of SMP membrane demonstrates a very strong vibration near the resonant frequency, which is not obvious at other excitation frequencies. For the case of the SMP membrane oscillating in a temperature-changing process, the amplitude of oscillation increases dramatically in the vicinity of the resonant-sensitive temperature. However, the oscillation amplitude reduces to a small value rapidly, as the temperature continues to rise. Heating rate also affects the maximum amplitude in the temperature-changing process. When the heating rate increases, the amplitude peaks become smaller, while the resonance temperatures barely change. From this study, the vibration of the SMP membrane could be controlled by properly regulating the heating rate. When the SMP membrane is driven by uniaxial sinusoidal force, the results are similar to the ones under equal-biaxial sinusoidal force, except that the maximal amplitudes are bigger and the resonance frequencies are lower. In the shape memory behavior of SMP membrane involving the dynamic response, the dynamic response has little influence on final shape fixation. But the shape recovery would be disturbed by the vibration. This work would provide a theoretical framework for predicting the dynamic behaviors of an SMP membrane and controlling the vibration of SMP membrane.

Acknowledgements. Authors are grateful for the support from the National Natural Science Foundation of China through Grant numbers 11572236, 11372236.

References

[1] Liu Z, Toh W, Ng TY. Advances in mechanics of soft materials: a review of large deformation behavior of hydrogels. Int J Appl Mech. 2015;7(05):1530001.
[2] Defossez M. Shape memory effect in tensegrity structures. Mech Res Commun. 2003;30(4):311–6.
[3] Yang H, Wang J, Liu Y. A new approach for the slope stability analysis. Mech Res Commun. 2001;28(6):653–69.
[4] Tobushi H, Okumura K, Hayashi S, Ito N. Thermomechanical constitutive model of shape memory polymer. Mech Mater. 2001;33(10):545–54.
[5] Yu K, Westbrook KK, Kao PH, Leng J, Qi HJ. Design considerations for shape memory polymer composites with magnetic particles. J Compos Mater. 2013;47(1):51–63.
[6] Lendlein A, Jiang H, Junger O, Langer R. Light-induced shape-memory polymers. Nature. 2005;434(7035):879.
[7] Leng J, Lan X, Liu Y, Du S. Electroactive thermoset shape memory polymer nanocomposite filled with nanocarbon powders. Smart Mater Struct. 2009;18(7):074003.

[8] Xiao R, Guo J, Safranski DL, Nguyen TD. Solvent-driven temperature memory and multiple shape memory effects. Soft Matter. 2015;11(20):3977–85.

[9] Hu J, Zhu Y, Huang H, Lu J. Recent advances in shape-memory polymers: structure, mechanism, functionality, modeling and applications. Prog Polym Sci. 2012;37(12):1720–63.

[10] Baghani M, Naghdabadi R, Arghavani J, Sohrabpour S. A thermodynamically-consistent 3D constitutive model for shape memory polymers. Int J Plast. 2012;35:13–30.

[11] Sokolowski WM, Tan SC. Advanced self-deployable structures for space applications. J Spacecr Rocket. 2007;44(4):750.

[12] Baghani M, Naghdabadi R, Arghavani J. A semi-analytical study on helical springs made of shape memory polymer. Smart Mater Struct. 2012;21(4):045014.

[13] Qiao T, Liu L, Liu Y, Leng J. Post buckling analysis of the shape memory polymer composite laminate bonded with alloy film. Compos Part B Eng. 2013;53:218–25.

[14] Lendlein A, Behl M, Hiebl B, Wischke C. Shape-memory polymers as a technology platform for biomedical applications. Expert Rev Med Dev. 2010;7(3):357–79.

[15] Ma M, Guo L, Anderson DG, Langer R. Bio-inspired polymer composite actuator and generator driven by water gradients. Science. 2013;339(6116):186–9.

[16] Hu J, Chen S. A review of actively moving polymers in textile applications. J Mater Chem. 2010;20(17):3346–55.

[17] Zhu Y, Hu J, Luo H, Young RJ, Deng L, Zhang S. Rapidly switchable water-sensitive shape-memory cellulose/elastomer nano-composites. Soft Matter. 2012;8(8):2509–17.

[18] Qi HJ, Nguyen TD, Castro F, Yakacki CM, Shandas R. Finite deformation thermo-mechanical behavior of thermally induced shape memory polymers. J Mech Phys Solids. 2008;56(5):1730–51.

[19] Li F, Liu L, Lan X, Wang T, Li X, Chen F. Modal analyses of deployable truss structures based on shape memory polymer composites. Int J Appl Mech. 2016;8(07):1640009.

[20] Kuang J, Meehan PA, Leung A, Tan S. Nonlinear dynamics of a satellite with deployable solar panel arrays. Int J Nonlinear Mech. 2004;39(7):1161–79.

[21] Qiu Z-c, Wu H-x, Zhang D. Experimental researches on sliding mode active vibration control of flexible piezoelectric cantilever plate integrated gyroscope. Thin Wall Struct. 2009;47(8):836–46.

[22] Zhong Y, Yin JH. Free vibration analysis of a plate on foundation with completely free boundary by finite integral transform method. Mech Res Commun. 2008;35(4):268–75.

[23] Baghani M, Arghavani J, Naghdabadi R. A finite deformation constitutive model for shape memory polymers based on Hencky strain. Mech Mater. 2014;73:1–10.

[24] Li Y, He Y, Liu Z. A viscoelastic constitutive model for shape memory polymers based on multiplicative decompositions of the deformation gradient. Int J Plast. 2017;91:300–17.

[25] Li Y, Hu J, Liu Z. A constitutive model of shape memory polymers based on glass transition and the concept of frozen strain release rate. Int J Solids Struct. 2017;124:252–63.

[26] Li Y, Guo S-S, He Y, Liu Z. A simplified constitutive model for predicting shape memory polymers deformation behavior. Int J Comput Mater Sci Eng. 2015;4(01):1550001.

[27] Sheng J, Chen H, Liu L, Zhang J, Wang Y, Jia S. Dynamic electromechanical performance of viscoelastic dielectric elastomers. J Appl Phys. 2013;114(13):034119.

[28] Zhang J, Tang L, Li B, Wang Y, Chen H. Modeling of the dynamic characteristic of viscoelastic dielectric elastomer actuators subject to different conditions of mechanical load. J Appl Phys. 2015;117(8):836.

[29] Liu Y, Gall K, Dunn ML, Greenberg AR, Diani J. Thermomechanics of shape memory polymers: Uniaxial experiments and constitutive modeling. Int J Plast. 2006;22(2):279–313. https://doi.org/10.1016/j.ijplas.2005.03.004.